

## HT-FED2004–56786

### Thermal, Electrical, and Mechanical Characterization of Carbon Nanotube–Epoxy Composites

Vivek Sundaram<sup>1</sup>, Roop L. Mahajan<sup>1</sup>

<sup>1</sup> Department of Mechanical Engineering,  
University of Colorado at Boulder,  
Boulder, CO 80309-0427  
[mahajan@spot.colorado.edu](mailto:mahajan@spot.colorado.edu)

Dudley S. Finch<sup>1,2</sup> and Stephanie A. Hooker<sup>2</sup>

<sup>2</sup> Materials Reliability Division  
National Institute of Standards and Technology  
Mailcode 853.00  
325 Broadway, Boulder, CO 80305-3328  
[finchd@boulder.nist.gov](mailto:finchd@boulder.nist.gov); [shooker@boulder.nist.gov](mailto:shooker@boulder.nist.gov);

#### ABSTRACT

Future microelectronic circuits will need to dissipate more than 100 Watts per chip for high-performance applications, posing a thermal-management challenge for the next generation of electronic packages [1, 2]. To meet this challenge, it is imperative that all interfaces, such as those between the chip and the heat spreader and between the heat spreader and the heat sink, introduce minimal thermal resistance. We propose the use of carbon nanotube–epoxy composites to provide enhanced heat dissipation at these critical junctions. Purified single-walled carbon nanotubes (SWNTs) are considered, and the matrix selected is a typical underfill epoxy used in flip-chip packaging. Three techniques were explored to embed the carbon nanotubes (CNTs) in the epoxy matrix, namely mechanical separation, mechanical dispersion in alcohol, and ultrasonic dispersion. The distribution of the nanotubes in the epoxy as the result of each technique was qualitatively determined by field-emission scanning electron microscopy (FE-SEM). Combining ultrasonic dispersion with mechanical mixing produced the most uniform distribution among the three approaches tested. As anticipated, the resulting composites showed enhanced thermal, electrical, and mechanical properties with increased nanotube content in the matrix. However, the increase in thermal conductivity was not as significant as the changes in electrical and mechanical behavior. To enable further improvements in heat dissipation, alignment of the nanotubes in the epoxy may be required. Development of such aligned composites may enable the use of lower CNT concentrations, allowing polymer ductility and electrical isolation to be preserved while reducing additive costs.

#### INTRODUCTION

Nearly 12 years ago, Sumio Iijima at NEC, Japan, first noticed odd nanoscopic threads lying in a smear of soot. Made of pure carbon, as regular and symmetric as crystals, these exquisitely thin, impressively long macromolecules soon became known as nanotubes [3, 4]. Carbon nanotubes (CNTs) can, in principle, play the same role as silicon in electronic circuits but at a molecular scale, where silicon and other

standard semiconductors cease to work [5, 6]. These materials exhibit unusually high thermal [7] and electrical conductivity [8, 9, 10], in addition to superior mechanical [11, 12] and optical behavior [13]. This unique combination of properties has prompted considerable research into CNT development and application. However, studies have revealed that the properties of CNTs are affected by impurities resulting from growth techniques [14] and by voids and vacancies formed due to the migration of atoms in the lattice structure [15]. As a result, the potential of CNTs for many applications has not yet been fully realized.

Recent advances and enhancements in the synthesis of nanotubes have made possible the growth of high-purity crystalline bundles of CNTs [16, 17]. In parallel, significant progress has also been made in determining the thermal properties of CNTs using both molecular dynamics simulations [18] and the physical measurement of thermal conductivity for an individual CNT attached to a MEMS platform [19].

In our research group, we are exploring the potential of carbon nanotube–epoxy composites for meeting the future thermal-management and interconnect requirements of electronic products. In this paper, the thermal, electrical and mechanical properties of various CNT composites have been measured and the effects of CNT concentration on performance determined.

#### NOMENCLATURE

$k$  – thermal conductivity,  $\sigma$  – electrical AC conductivity,  $E$  – Young's Modulus

#### SPECIMEN PREPARATION

Carbon nanotubes were purchased from a commercial supplier [20] and specified by the manufacturer to be predominantly single-walled. The epoxy selected was a common underfill polymer used in flip-chip packages [21]. It contains approximately 70% filler material, which reduces the effective coefficient of thermal expansion of the epoxy and enables thermal compatibility with common substrates and solders. The filled polymer is designed to flow readily in order

to facilitate penetration of gaps as small as 25  $\mu\text{m}$  (1 mil) under a chip, and, when fully cured, it forms a rigid, low-stress seal.

Three techniques were explored to embed the nanotubes in the epoxy, namely mechanical separation, mechanical dispersion in alcohol, and ultrasonic dispersion. The effectiveness of each for dispersing the CNTs was evaluated using high-resolution Field-Emission Scanning Electron Microscopy (FE-SEM). Electron micrographs for each method are shown in Figure 1(a) – 1(c). All specimens evaluated have 1 percent by weight of CNT in epoxy. Several locations across each specimen were examined, and two randomly selected areas are shown in the following figures.

In Figure 1(a), we observe that the two portions of the specimen show very different nanotube distributions when only a mortar and pestle were used to mix the two materials. On the right, a cluster of CNTs is visible, while the area on the left is completely devoid of CNTs. Similarly, the SEM micrographs in Figure 1(b) again illustrate non-uniform distribution when the materials were mechanically mixed in alcohol. However, in Figure 1(c), nanotubes were found in all regions examined, indicating better distribution. Nevertheless, it should be noted that because of the high filler content in the initial epoxy, highly uniform distributions may be difficult to achieve.

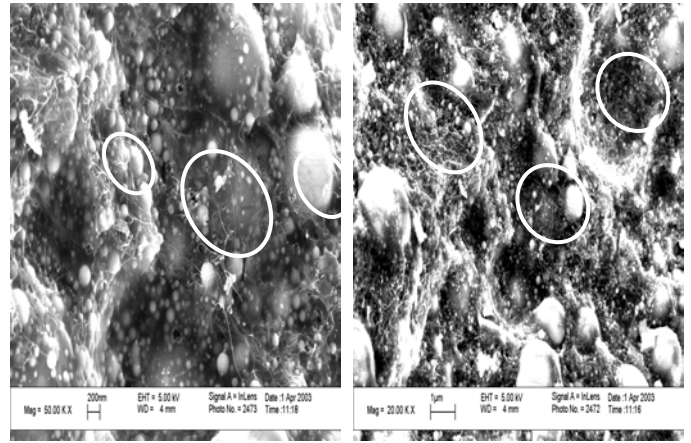


Figure 1(c): Random portions of a typical specimen prepared by a combination of mechanical mixing and ultrasonic dispersion. Clusters of nanotubes (circled) were found in all portions of the specimen, indicating better distribution as compared to the previous two approaches.

Based on these qualitative SEM analyses, the following preparation procedure was then used to produce a series of CNT composites for performance characterization. First, the nanotubes were mechanically crushed and separated using a mortar and pestle, followed by ultrasonic dispersion for up to two hours in methanol. The alcohol was then allowed to evaporate overnight leaving a black residue of carbon particles behind. This alcohol-free CNT residue was subsequently mixed with the epoxy mechanically using a mortar and pestle to ensure uniform dispersion. The uncured composite mixture was then transferred to specially-fabricated, flexible silicone rubber molds of varying sizes (shown in Figure 2) to obtain test specimens of suitable dimensions. The molds were first placed in an oven under vacuum and held at 75  $^{\circ}\text{C}$  for 20 minutes to remove trapped air from the mixture. Specimens were then soaked at 150  $^{\circ}\text{C}$  for two hours to obtain fully-cured composites.

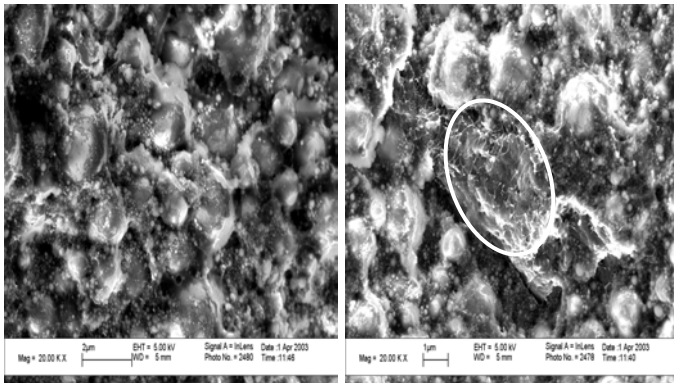


Figure 1(a): Random portions of a typical specimen prepared by mixing the materials with a mortar and pestle. The left micrograph illustrates a region devoid of nanotubes, while the right shows several nanotube clusters (one of which is circled).

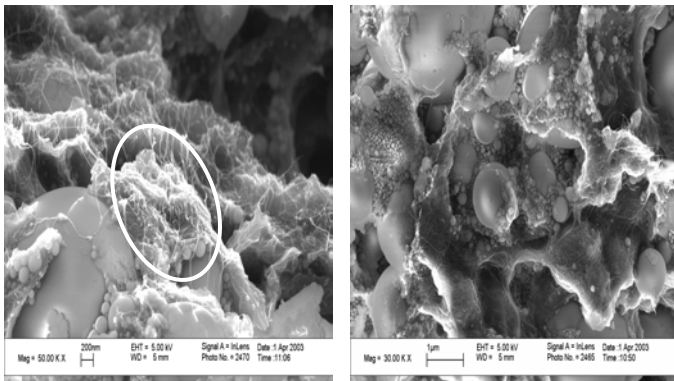


Figure 1(b): Random portions of a typical specimen prepared by manually stirring the nanotubes into epoxy dissolved in alcohol. Several nanotube clusters are visible in the left micrograph (one of which is circled), while no nanotubes were located in the region in the right micrograph.

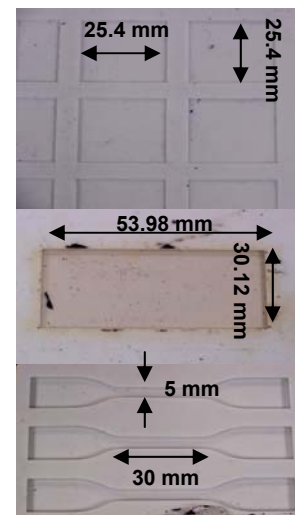


Figure 2: Specially-fabricated silicone molds used for preparing composite specimens.

The mold configurations were as follows: (1) dog-bone-shaped specimens of dimensions 30 mm x 5 mm x 3 mm for tensile testing; (2) squares of dimensions 25.40 mm x 25.40 mm x 0.99 mm for electrical characterization; and (3) plates of dimensions 53.98 mm x 30.12 mm x 1.41 mm for use as an interface material during thermal testing.

### EFFECT ON CURE KINETICS

Next, isothermal Dynamic Scanning Calorimetry (DSC) was performed to investigate the effect of the CNT additions on the curing reaction of the polymer matrix. The epoxy came in syringes which were stored at -100 °C in a deep freezer. At this low temperature, the epoxy is in a glassy state. The curing reaction is diffusion-controlled and, therefore, extremely slow to occur. Thus, it can be safely assumed that the epoxy was initially uncured. Five milligrams of epoxy was used as the base matrix for each DSC run and was mixed with 0, 0.5, 1, 2, 4, and 5 weight percents of carbon nanotubes. The epoxy was cured in-situ in the DSC by heating at a constant rate of 40 °C/min from room temperature to 150 °C and holding at 150 °C for 2.5 hours during which time the curing reaction took place. This temperature was consistent between all CNT loadings. The specimens were then cooled at a constant rate of 40 °C/min to room temperature. No changes in the kinetics of the curing reaction were observed due to the addition of carbon nanotubes to the polymer matrix.

### ELECTRICAL CONDUCTIVITY MEASUREMENTS

To evaluate the electrical performance of the composites, the DC resistance of each specimen was first measured using a digital multimeter to determine if the specimens were electrically conductive. Next, a 2-terminal AC impedance measurement was performed to evaluate the electrical behavior of the different materials as a function of frequency. In this measurement, an impedance analyzer was used to acquire data on both the real and imaginary parts of the complex impedance ( $Z^*$ ) and admittance ( $Y^*$ ) from 100 Hz to 1 MHz. AC conductivity was then calculated for each specimen using the following formula:

$$\sigma = \frac{Y' \times d}{A} \quad (1)$$

where  $Y'$  is the real part of the complex admittance,  $d$  is the distance between electrodes (i.e., the average thickness), and  $A$  is the electrode area. Electrodes (1 cm<sup>2</sup>) were manually applied to the top and bottom surfaces of each specimen using a conductive silver-epoxy paste, which was subsequently cured for 30 minutes at 100 °C. Electrical leads were then attached to each electrode for measurement. The impedance analyzer was compensated internally for the resistance of these leads, as well as for that of the measurement fixture. Compensation was performed prior to each test to reduce measurement error. Based on previous studies using known resistors, the error associated with these measurements is less than +/- 5%. DC measurements resulted in resistances greater than 50 MΩ (i.e., the measuring limit of the multimeter) for 0 and 0.5 weight-percent specimens. For 1, 2, 4 and 5 weight-percent CNT samples, the resistances were approximately 7 MΩ, 1 MΩ,

20 kΩ and 5 kΩ respectively, with the resistance decreasing with increasing CNT concentration.

A similar trend was revealed by the AC measurements. A plot of the AC conductivity as a function of frequency is shown in Figure 3. The conductivity was calculated at different frequencies ranging from 100 Hz to 1 MHz. The 0.5 and 1 weight-percent composites behaved similarly to the unreinforced matrix, with conductivity increasing with increasing frequency. Such behavior is typical of insulators. However, once the percentage of CNTs was increased above 1 percent, the conductivity no longer varied with frequency, indicating that the percolation threshold had been reached and that the specimens were conductive.

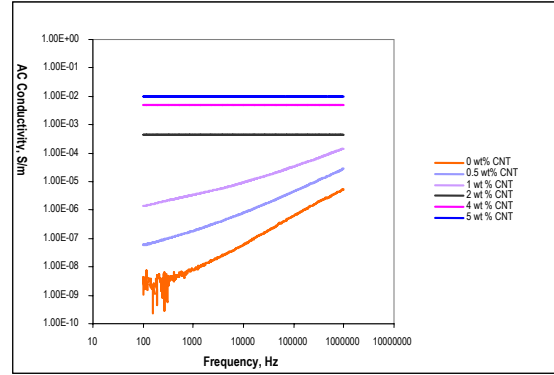


Figure 3: Effect of frequency on electrical conductivity for different weight percentages of CNTs in epoxy.

Examining the results at 1 kHz, as shown in Figure 4, the increase in conductivity becomes asymptotic at approximately 4 weight percent. At 5 weight percent, the conductivity improves only slightly, indicating that the effect due to the reinforcement is nearing saturation.

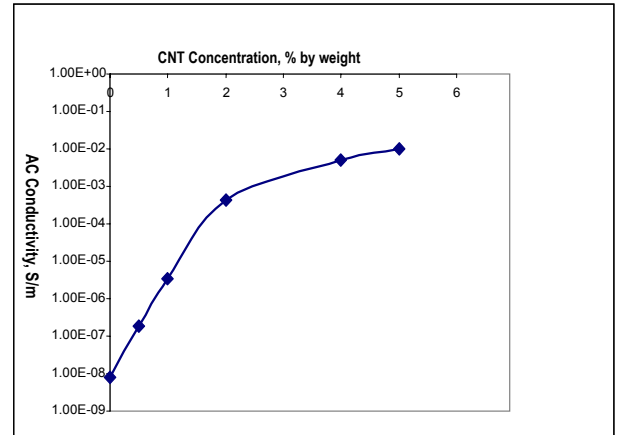


Figure 4: Variation of electrical conductivity at 1 kHz as a function of CNT concentration in the matrix.

### THERMAL CONDUCTIVITY MEASUREMENTS

As in the electrical measurements, specimens containing 0, 0.5, 1, 2, 4 and 5 percent CNTs were fabricated for thermal conductivity testing. A sandwich experiment similar to that described in ASTM standard C177-97 [22] was employed using a constant input power of 13 Watts. The experimental setup, as shown in Figure 5, included a solid aluminum block of



dimensions 53.98 mm x 30.12 mm x 76.20 mm. This block weighed approximately 600 g, and a patch heater was attached to its top side. Thermocouples were also attached at three equidistant locations, namely 6.35 mm, 38.10 mm, and 69.85 mm from the top end of the aluminum block. A 127 mm<sup>2</sup> square copper plate was maintained at 8°C by circulating water from a constant temperature bath. The weight exerted by the aluminum block helped minimize air gaps between the aluminum and the specimen and the specimen and the copper plate, thereby reducing contact resistance.

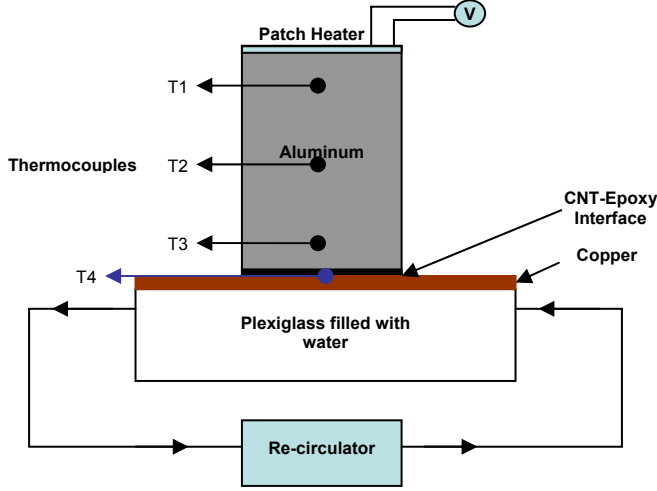


Figure 5: Schematic of the thermal conductivity setup.

In a typical run, the copper plate is first cooled down to 8 °C by circulating water through the plexiglass enclosure. After allowing the cooled plate to reach thermal equilibrium, the patch heater is then switched on and set to a constant input power. Once steady state conditions are again reached, the temperatures are recorded from thermocouples T1, T2, T3, and T4. The temperature, T3, is extrapolated to the tip of the aluminum at the junction between the aluminum and the composite. This temperature is denoted as  $T3'$ . Because the temperature, T4, is measured on the surface of the copper plate, it is directly used to calculate the change in temperature as follows:

$$\Delta T = T3' - T4 \quad (2)$$

The thermal conductivity of the interface is then calculated using the relation:

$$k = \frac{Q \times l}{A \times \Delta T} \quad (3)$$

where  $l$  is the thickness of the composite interface, which in this case equals 1.41 mm.

The results are plotted in Figure 6. We note that the value of  $k$  obtained in Eq. (3) is a measure of the overall conductance and includes contact resistance at the two interfaces. However, the measured value for the pure epoxy in this experiment (0.86 W/m-K) compares well with the values reported previously in the literature (0.87 W/m-K) [23], indicating that the thermal

resistance can be considered to be negligible. Assuming that in the subsequent tests at different CNT concentrations the thermal interface resistance remains the same, it is fair to take the  $k$  values determined through Eq. (3) as the accurate estimates of thermal conductivity.

The thermal conductivity was found to increase with increasing CNT loading. At 5 weight percent CNT, the thermal conductivity of the composite is approximately 200% of that of the matrix. The drop experienced from 0 ( $k=0.87$  W/m-K, thermal conductivity of pure matrix) to 0.5 weight percent ( $k=0.58$  W/m-K) is thought to be an anomaly. We believe that this drop is due to the presence of air bubbles trapped during composite preparation due to the introduction of CNTs in the continuous, rigid crosslinks of the thermoset epoxy.

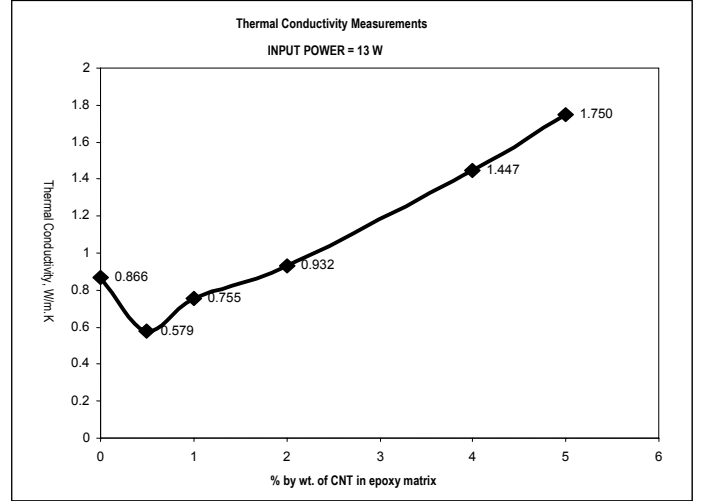


Figure 6: Thermal conductivity vs. CNT concentration.

We also note that the CNTs are randomly oriented in the matrix and do not provide a continuous thermal path. As a result, the potential thermal conductivity improvement may not have been fully realized.

## MECHANICAL PROPERTY MEASUREMENTS

Tensile tests of dog-bone-shaped specimens were performed at room temperature (21 °C) at a constant cross-head speed of 1 mm/min on a standard electro-mechanical tester. The resulting strain was measured with an extensometer. The gauge length was 12.5 mm  $\pm$  2.5 mm, and the thickness of each specimen was 3 mm. Most tests were performed to the limit strain of the extensometer with the exception of the 4 and 5 weight-percent specimens, which broke below that limit. The stress-strain curves for the various specimens are shown in Figure 7.

As seen in the Figure 7, the epoxy resin is quite ductile, and the maximum stress levels reached are considerably lower than those of standard epoxy resins (i.e., 30-60 MPa). The yield strength increased with increasing CNT reinforcements in the matrix. The mechanical properties of 0, 1, 2, 4 and 5 weight percent specimens are presented in Table 1. Normalized stress-strain curves presented in Figure 8 show a better representation of the effect of CNT additions on mechanical behavior. In this figure, the stress of the composite matrix with different CNT concentrations is divided by the pure

matrix stress at the same strain level. It can again be concluded that the effect of CNT reinforcements begins to taper off at 4 weight percent. A similar trend is observed for Young's modulus, as shown in Figure 9.

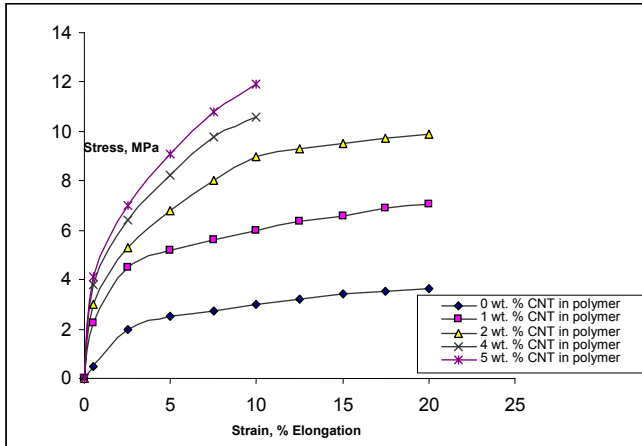


Figure 7: Stress-strain relationships for the bare resin and various CNT composites as determined by tensile testing.

Table 1: Young's Modulus and yield strength at 10% strain.

CNTs in matrix (wt. %)	Young's Modulus (MPa)	Yield Strength at 10% elongation (MPa)
0	$E_0 = 109$	3.0
1	$E_1 = 235$	6.0
2	$E_2 = 348$	9.0
4	$E_4 = 396$	10.6
5	$E_5 = 432$	11.9

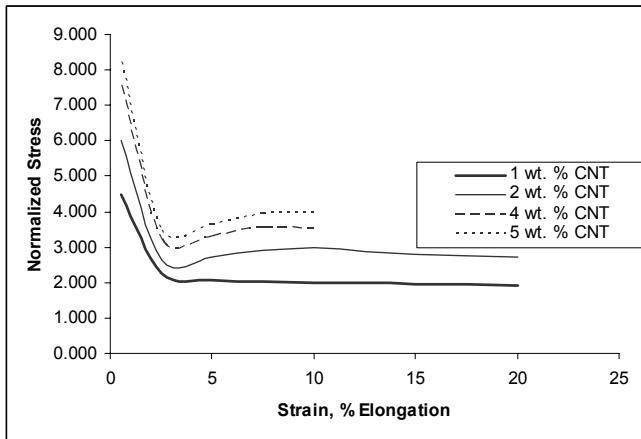


Figure 8: Normalized stress-strain curves for resin composites.

The distinct change in mechanical behavior at higher CNT concentrations is likely due to the contribution of the additive (which is more brittle than the polymer) beginning to outweigh the contribution of the matrix. However, it should be noted that porosity variations may also influence the mechanical properties. The SEM images in Figure 1(b) show the presence

of large pores, likely due to air bubbles trapped in the epoxy during mixing. Porosity can also occur at the interface between the nanotubes and epoxy due to incomplete mixing. As the fraction of nanotubes increases, this interfacial porosity will also increase, contributing to the relative brittleness of these highly-loaded composites.

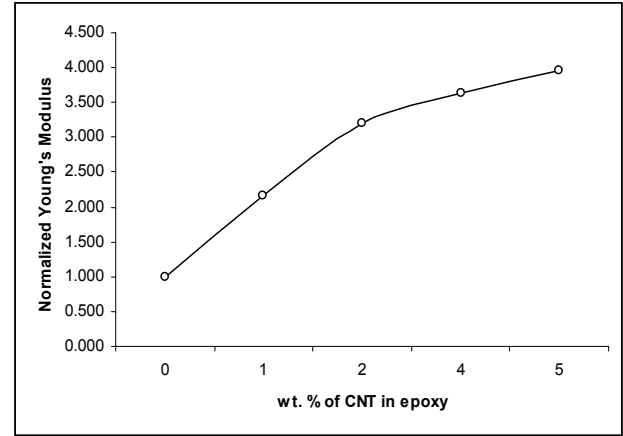


Figure 9: Normalized Young's modulus of CNT-epoxy composites at 10% elongation.

## CONCLUSIONS

The results from thermal, mechanical, and electrical characterization demonstrate the potential of using carbon nanotubes as reinforcements for electronic packaging materials. It has been observed that even small CNT additions can markedly alter the properties of the base polymer. In particular, the electrical measurements show that conductivity increases significantly with increasing CNT concentration, with the effect more pronounced for lower weight percentages. Percolation (i.e., the point at which a conductive, interconnected network is formed) was reached at 2 weight percent. Due to the lack of a continuous thermal path across the thickness of the specimen, and due to the random orientation of CNTs in the matrix, the thermal conductivity increase was not as substantial. At 5 weight percent CNT, the thermal conductivity increased by only a factor of two. Nanotube additions also had a considerable effect on the mechanical properties, with Young's modulus and yield strength increasing by approximately 100 and 200% respectively with only 1 weight percent CNT added. The decrease in the slope of the normalized Young's modulus curve (Figure 9) at higher weight percentages confirms that the homogeneity of the composite is critical for optimizing mechanical behavior, whereas inhomogeneity may have less of an effect on electrical properties.

The results of this study indicate that it would not be helpful to use high concentrations of carbon nanotubes to improve the properties of the underfill material if they are randomly oriented in the matrix. Alignment of the tubes in the epoxy may be needed to improve heat dissipation without further sacrificing ductility or electrical isolation.

## ACKNOWLEDGEMENTS

The authors acknowledge the financial and technical support offered by Dr. Suraj Rawal from Lockheed Martin. We also gratefully acknowledge the support provided by the

Bowman lab group at the Department of Chemical Engineering, University of Colorado, Boulder, for their DSC equipment. The authors would also like to thank the National Institute of Standards and Technology for their invaluable support toward providing instrumentation and equipment to perform the various tests for successful completion of this paper.

## REFERENCES

- [1] Li, H., Jacob, K.I., and Wong, C.P., *An Improvement of Thermal Conductivity of Underfill Materials for Flip-Chip Packages*. IEEE Transactions on Advanced Packaging, **26**(1), 25 (2003).
- [2] M.Arik, *Ebullient Cooling of Electronics: Future Trends and Recent Advances*. PTC-03 International Short Course on Passive Thermal Control, held October 22-24, 2003, Antalya, Turkey.
- [3] Dresselhaus M.S., Dresselhaus G., and Eklund P.C., *Science of Fullerenes and Carbon Nanotubes*. London: Academic Press (1996)
- [4] Iijima S., *Helical microtubules of graphite carbon*. Nature (London) (1991), 354:56-8.
- [5] Frank S., Poncharal P., Wang Z.L., and De Heer W.A., *Carbon Nanotube Quantum Resistors*. Science **280**, 1744 (1998)
- [6] Sanvito S., Kwon Young-Kyun, Tomanek D., and Lambert C.J., *Fractional Quantum Conductance in Carbon Nanotubes*. Phys. Rev. Lett. **84**(9), 1974 (2000)
- [7] Berber S., Kwon Young-Kyun, and Tomanek D., *Unusually High Thermal Conductivity of Carbon Nanotubes*. Phy. Rev. Lett. **84**(20), 4613 (2000)
- [8] Jeon Tae-In, Kim Keun-Ju, Kang C., Oh Seung-Jae, Son Joo-Hiuk, An K.H., Bae D.J, and Lee Y.H., *Terahertz Conductivity of Anisotropic Single-walled Carbon Nanotube Films*. App. Phy. Lett. **80**(18), 3403 (2002)
- [9] Sandler J., Shaffer M.S.P., Prasse T., Bauhofer W., Schulte K., and Windle A.H., *Development of a dispersion process for Carbon Nanotubes in an Epoxy matrix and the resulting Electrical Properties*. Polymer **40**, 5967 (1999)
- [10] Grimes C.A., Mungle C., Kouzoudis D., Fang S., and Eklund P.C., *The 500 MHz to 5.50 GHz complex Permittivity spectra of Single-wall Carbon Nanotube-loaded polymer composites*. Chem. Phy. Lett. **319**, 460 (2000)
- [11] Yu Min-Feng, Files B.S., Arepalli S., and Ruoff R.S., *Tensile Loading of Ropes of Single-walled Carbon Nanotubes and their Mechanical Properties*. Phy. Rev. Lett. **84**(24), 5552 (2000)
- [12] Krishnan A., Dujardin E., Ebbesen T.W., Yianilos P.N., and Treacy M.M.J., *Young's Modulus of Single-walled Nanotubes*. Phy. Rev. B **58**(20), 14013 (1998)
- [13] Kymakis E., Alexandou I., and Amaratunga G.A.J., *Single-walled Carbon Nanotube-Polymer Composites: Electrical, Optical and Structural Investigation*. Synthetic Metals **9108**, 1-4 (2001)
- [14] Che J., Cagin T, and Goddard III W.A., *Thermal Conductivity of Carbon Nanotubes*. Nanotechnology **11**, 65-69 (2000)
- [15] Nardelli B.M., Fattebert J.L., Orlikowski D., Roland C., Zhao Q., and Bernholc J., *Mechanical Properties, Defects and Electronic Behavior of Carbon Nanotubes*. Carbon **38**, 1703-1711 (2000)
- [16] Sohn J.I., Choi Chel-Jong, Lee S., and Seong Tae-Yeon, *Growth Behavior of Carbon Nanotubes on Fe-deposited (001) Si substrates*. App. Phy. Lett. **78**(20), 3130 (2001)
- [17] Huang Z.P., Xu J.W., Ren Z.F., Wang J.H., Siegal M.P., and Provencio P.N., *Growth of highly oriented Carbon Nanotubes by plasma-enhanced hot filament chemical vapor deposition*. App. Phy. Lett. **73**(26), 3845 (1998)
- [18] Prylutsky Y.I., Durov S.S., Ogloblya O.V., Buzaneva E.V., and Scharff P., *Molecular dynamics simulation of Mechanical, Vibrational and Electronic properties of Carbon Nanotubes*. Computational Materials Science **17**, 352-355 (2000)
- [19] Kim P., Shi L., Majumdar A., and McEuen P.L., *Thermal Transport Measurements of Individual Multiwalled Nanotubes*. Phy. Rev. Lett. **87**(21), 5021 (2001)
- [20] Carbon Nanotechnologies, Houston, TX.
- [21] Hysol FP4511, Loctite Corporation.
- [22] *Standard Test Method for Steady-State Heat Flux Measurements and Thermal Transmission Properties by Means of the Guarded-Hot-Plate Apparatus*, ASTM-C177-97.
- [23] Mahajan R.L., Malhotra C.P., and Sharma R.K., *An Analytical Cure Model for underfill epoxies*, ASME J. Electronic Packaging, **124**, 391-396 (2002).